A&A 397, 7–13 (2003)
DOI: 10.1051/0004-6361:20021473


Astronomy & Astrophysics

# Ly-$\alpha$ photon induced amorphization of Ic water ice at 16 Kelvin

## Effects and quantitative comparison with ion irradiation

G. Leto and G. A. Baratta

INAF, Osservatorio Astrofisico di Catania, Via S. Sofia 78, 95123 Catania, Italy

Received 27 June 2002 / Accepted 7 October 2002

**Abstract.** Water ice is a ubiquitous material in space, on the surface of planets and their moons, in comets and interstellar dust grains. The structure of water ice strongly depends on the deposition temperature. It can be amorphous if deposited at low temperature, i.e. 16 K, or crystalline if the deposition temperature is higher than 140 K. In this paper we report the first experimental study of the structural effects induced by Lyman-$\alpha$ UV photons in crystalline water ice carried out by in situ infrared spectroscopy. The effects induced by Lyman-$\alpha$ photolysis are compared with those induced by ion irradiation carried out with the same experimental apparatus. We found that, as already observed in the case of fast ions, also UV Lyman-$\alpha$ photons are able to fully amorphize the crystalline water ice structure after a dose of few eV per molecule. This study has important astrophysical implications, in particular because photons and fast ions are both present in space, they can induce variations in the profile of the 3 $\mu$m band of crystalline water ice. Thus these effects have to be considered when one attempt to deduce information on the physical status (e.g. temperature history) of the responsible dust from the profile of the observed ice band.

**Key words.** astrochemistry – molecular processes – methods: laboratory – techniques: spectroscopic – ISM: molecules

## 1. Introduction

Different forms of water ice exist depending on the deposition rate and substrate temperature. If the deposition of water vapor is made at temperatures between 140 and 150 K, crystalline cubic ice (Ic) is produced. Crystalline cubic ice is stable under cooling, but if heated, to about 200 K, it is converted to crystalline hexagonal ice (Ih). When vapor is deposited at temperatures below ~100 K the resulting ice is amorphous (P/ASW, Porous/Amorphous Solid Water). It is possible to obtain several forms of amorphous water ice (Boutron & Alben 1975; Hagen et al. 1983; Jenniskens et al. 1995); some of the sensible parameters are: substrate temperature and nature, deposition rate, deposition flow angle (Westley et al. 1998; Devlin 2001). P/ASW once formed is unstable against temperature cycling: as $T$ increases it is converted to crystalline ice on a time scale which depends exponentially on $T$ (Schmitt et al. 1989); at 150 K it is shorter than 10 s, at 20 K it is longer than the age of the Universe (Schmitt et al. 1989).

Water ice has a well-known infrared spectrum that exhibits bands due to O-H stretching and bending modes at 3 $\mu$m and 6 $\mu$m respectively, the libration band at 12 $\mu$m, a band at 4.5 $\mu$m attributed to the combination of bending and libration, and a lattice band at 45 $\mu$m. Because of the asymmetry at the surface or inside pores, small bands arise from molecules that do not saturate their possible bonds, so H and O dangling bonds appear in the 2.7–2.8 $\mu$m range.

The shapes of the infrared absorption features of water ice strongly depend on the structure of the ice. As an example, Fig. 1, shows the 3-micron band (the most intense in the mid IR) for cubic ice obtained by depositing $H_2O$ vapor at 150 K and cooling to 16 K, and for an amorphous ice sample of the same thickness directly deposited at 16 K. Their profiles (peak position, shape, strength) are very different. Thus IR spectroscopy in the 3-micron region is a good technique to investigate structural changes of water ice.

If only equilibrium thermal processes are considered, the observation of infrared features of P/ASW ice in several astronomical objects would imply that the ice is formed directly at low $T$, and it has never experienced temperature increases since the epoch of its formation. However experiments carried out on crystalline (cubic) ice (Baratta et al. 1991; Strazzulla et al. 1992; Moore et al. 1992) showed that the transition from crystalline to amorphous water ice can be induced by keV-MeV ion irradiation at temperatures between 10 and 100 K. It was found that at low temperatures ($T < 55$ K) the process is very efficient (few eV/molec are sufficient to amorphize the ice) and at $T < 20$ K the profile of the 3-micron band of ion-irradiated crystalline water ice is close to the band of amorphous ice deposited at the same temperature. At higher temperatures ($T > 55$ K) the fraction of amorphous water ice

*Send offprint requests to*: G. Leto, e-mail: gle@ct.astro.it

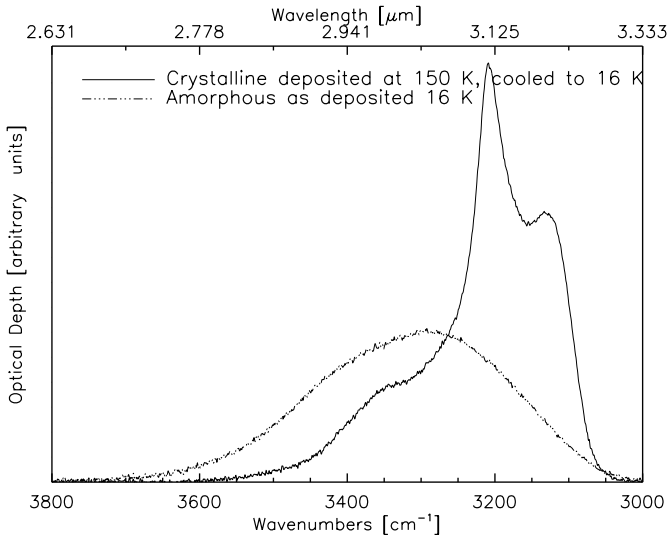


**Fig. 1.** The 3-micron OH band in the case of crystalline and amorphous water ice.

obtained after irradiation is reduced and the crystalline water ice becomes more resistant (greater doses are needed to disorder the structure). Similar results (Lepault et al. 1983; Heide 1984; Dubochet & Lepault 1984) have been found for high energy electron irradiation of thin layers of ice crystals below 70 K. Another process for the transformation from cubic to amorphous ice was reported by Kouchi & Kuroda (1990). Photons from a deuterium lamp (<11.3 eV) converted cubic ice into amorphous ice at a temperature below 70 K as evidenced by in situ reflection electron diffraction. However that result has been questioned (Jenniskens et al. 1995) because the reported fluence ($3 \times 10^{13}$ photons/cm$^2$) corresponds to a dose of $6 \times 10^{-5}$ eV/molec that is a strikingly low value.

In this paper we describe an experimental study of the effects induced by UV photolysis in crystalline water ice (Ic). For the first time, a quantitative description of the structural effects induced by UV Ly-$\alpha$ photons in water-ice is given; the effects are compared with those induced by ion irradiation in the same experimental setup. In Sect. 2 we describe our experimental apparatus and procedures, in Sect. 3 a description of the full set of experiments and irradiation parameters is reported. The results are presented in Sect. 4 and discussed in Sect. 5. Summary and concluding remarks are reported in Sect. 6.

## 2. Experimental setup

The experimental work reported in this paper has been carried out in our laboratory at Catania Astrophysical Observatory. The experimental setup allows in situ IR spectroscopy of frozen gases and refractory materials irradiated with fast ions and Lyman-$\alpha$ photons.

### 2.1. Infrared spectroscopy

The in situ IR spectroscopy is performed in a stainless steel vacuum chamber (see Fig. 2) facing an FTIR spectrometer (Bruker Equinox 55). Inside the vacuum chamber the pressure

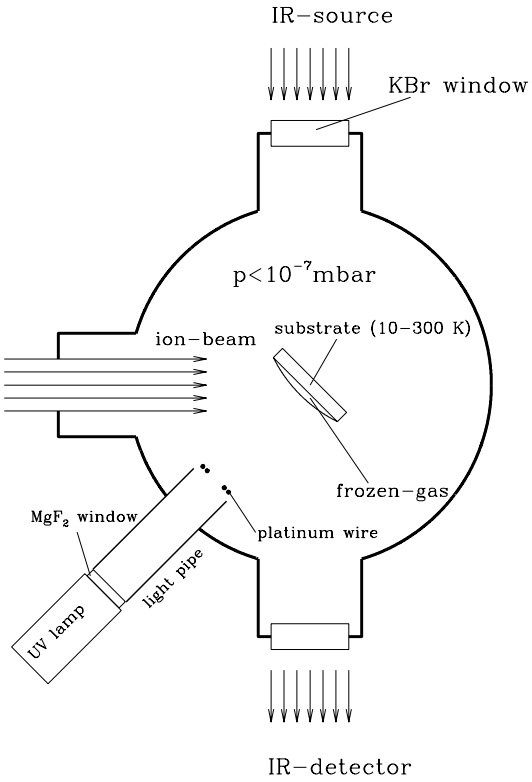


**Fig. 2.** Schematic view of the experimental apparatus used for in situ IR spectroscopy of ion and UV photolyzed frozen gases.

is kept below $10^{-7}$ mbar. An IR transparent substrate (crystalline silicon) is placed in thermal contact with a cold finger whose temperature can be varied between 10 K and 300 K. A needle valve is used to admit pre-prepared gases (or mixtures) into the chamber where they freeze on the substrate. The thickness of the ice film can be controlled, during deposition, by looking at the interference pattern (intensity versus time) given by a He-Ne laser beam reflected at an angle of 45 deg both by the vacuum-film and film-substrate interfaces (see Baratta & Palumbo 1998, for further details on the technique used to measure thickness). The substrate holder forms a 45 deg angle with both the IR beam and the ion beam and it is orthogonal to the UV beam. In this way, spectra can be easily taken in situ, even during irradiation with ions and UV photolysis, without tilting the sample. For this purpose the IR spectrometer is positioned (by a movable optical bench) so that the IR beam is transmitted by the substrate through a hole in the sample holder. In the experiments here reported the structural evolution under irradiation of deposited water ices is followed by monitoring the 3 $\mu$m OH stretching band. The spectra reported in the next sections have been acquired at oblique incidence (45°) with the electric vector perpendicular (s polarized) to the plane of incidence. The plane of incidence is the plane of the paper in Fig. 2; this plane contains the electric vector of p polarized light while the plane of s polarization is perpendicular to the paper. As already shown (see Baratta et al. 2000) spectra taken at oblique incidence in s polarization are equivalent to unpolarized spectra at normal incidence.

### 2.2. Ion and UV irradiation subsystems and calibration

The ion implanter is a 30 kV accelerator from which ions with energy up to 30 keV (60 keV for double ionizations) can be obtained. The ion beam produces a $2 \times 2$ cm$^2$ spot on the target and current ranges between 100 nA/cm$^2$ and tens of $\mu$A/cm$^2$.

A hydrogen microwave discharge resonance lamp (Opthos Instruments), capable of producing 10.2 eV photons, is interfaced to the vacuum chamber through a $MgF_2$ window. An aluminum light collector is placed at the end of the lamp in order to increase the number of UV photons that reach the sample. The UV flux given by a microwave powered discharge lamp strongly depends on the operating conditions and can vary over one order of magnitude. We have developed a monitoring system of the UV flux in order to have a reliable measure of the total number of UV photons that reaches the sample during photolysis. This was obtained by measuring the current given by photoelectric effect on a platinum wire placed at the end of the aluminum light collector. The total charge measured by the wire detector is proportional to the total UV photon number per square centimeter that reached the sample (fluence). The calibration constant of the wire was determined by measuring the $O_2 \rightarrow O_3$ conversion rate in a UV photolyzed $O_2$ ice film (see Gerakines et al. 1996; Gerakines et al. 2000) (see Baratta et al. 2002, for further details).

Photolysis of frozen $O_2$ slab with Lyman-$\alpha$ photons produces ozone ($O_3$) with a yield of 1.92 [molecule/Ly-$\alpha$ photon] (Groth 1937; Gerakines et al. 2000). In order to ensure that almost all the incoming Ly-$\alpha$ photons are absorbed in the slab we deposit a 1 $\mu$m thick $O_2$ layer at 16 K. The ozone production was monitored via the 1040 cm$^{-1}$ band assuming that the band strength is $1.4 \times 10^{-17}$ [cm/molecule] as measured in the gas phase 1985. The number of impinging Ly-$\alpha$ photons is evaluated through the amount of $O_3$ produced during the initial linear phase.

The ratio between the photon fluence measured with the Ozone method and the integrated wire current, has been verified to be constant within the whole range of flux provided by the lamp ($10^{12}$–$5 \times 10^{14}$ photons cm$^{-2}$ s$^{-1}$).

## 3. Ion irradiation and Lyman-$\alpha$ photolysis of crystalline $H_2O$

One of the objectives of this work was to verify if Ly-$\alpha$ photons were able to induce amorphization of Ic $H_2O$ at low temperature. This was achieved by looking at the 3 $\mu$m band profile evolution during Ly-$\alpha$ photolysis; the band profile evolution was compared with that observed for fast ions ($H^+$, $He^+$, $Ar^{++}$) irradiation performed in the same experimental setup.

In the case of ion irradiation the dose has been calculated from the knowledge of the stopping power (eV cm$^{-2}$ molecule$^{-1}$, computed by using the TRIM Montecarlo simulation program) and of the integrated ion flux (ions cm$^{-2}$), which is directly related to the integrated ion current. In the case of Ly-$\alpha$ photons the energy released per molecule can be evaluated once the total number of absorbed photons is known.

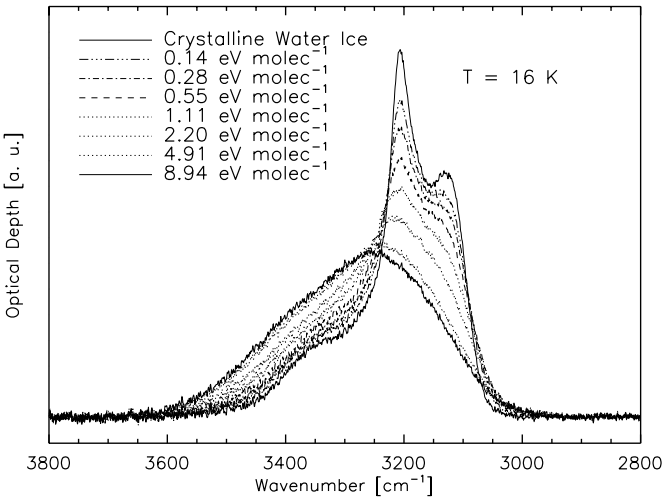


**Fig. 3.** Evolution of the crystalline water ice band under UV photolysis.

The number of Ly-$\alpha$ photons absorbed by the irradiated sample depends on the thickness of the sample and on its absorption coefficient. The absorption law can be described by an exponential of the type $I = I_o\, e^{-ad}$, where a is the absorption coefficient and d is the thickness. We have evaluated the absorption coefficient for Ly-$\alpha$ photons in water ice making different experiments in which we used samples with different thickness. We have found an absorption coefficient for water ice of 28 $\mu$m$^{-1}$ (the full description of this method can be found in Baratta et al. 2002). The imaginary part of the refractive index of water ice at $\lambda = 0.121$ $\mu$m is $m_{\rm im} = 2.47 \times 10^{-1}$ (see Warren 1984). By using the relation $a = 4 \times \pi \times m_{\rm im}/\lambda$ we obtain $a = 26$ $\mu$m$^{-1}$, that is close to our measure. In our experiments the ice film thickness was about 500 Å so that the ice sample is fully processed by photons through the whole thickness. The dose has been calculated from the knowledge of the integrated flux (photons cm$^{-2}$) of impinging photons measured by the wire detector during the experiment and of the percentage of impinging UV photons absorbed in the sample (estimated by using the measured absorption coefficient). The ratio between the energy absorbed by the ice in eV/cm$^2$ (number of absorbed UV photons/cm$^2$ multiplied by 10.2 eV) and the number of water molecules/cm$^2$ gives the irradiation dose in eV/molecule.

## 4. Ion irradiation and Ly $\alpha$ photolysis: Results

### 4.1. UV photolysis

Figure 3 shows the evolution of the 3-micron band of a water ice Ic sample at 16 K photolyzed by 10.2 eV Lyman-$\alpha$ photons. The band profile at the end of photolysis is close to that of an amorphous sample having the same thickness. Few eV/molecule (~5) are enough to complete the process. Figure 4 shows four spectra: as deposited amorphous ice (16 K), Ic ice sample (16 K), and the spectra of the same samples but after UV photolysis. The two last spectra are so similar to be hardly distinguishable in the figure.

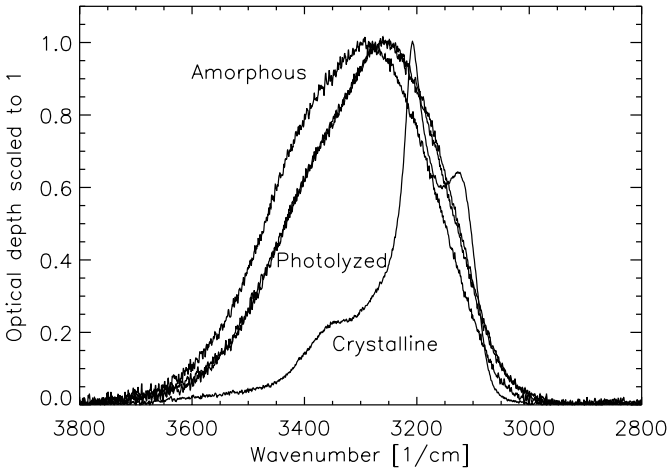


**Fig. 4.** Spectra of a crystalline and of an amorphous water ice sample at 16 K; the spectra of the same samples after UV photolysis are also shown. The photolyzed spectra are hardly distinguishable.

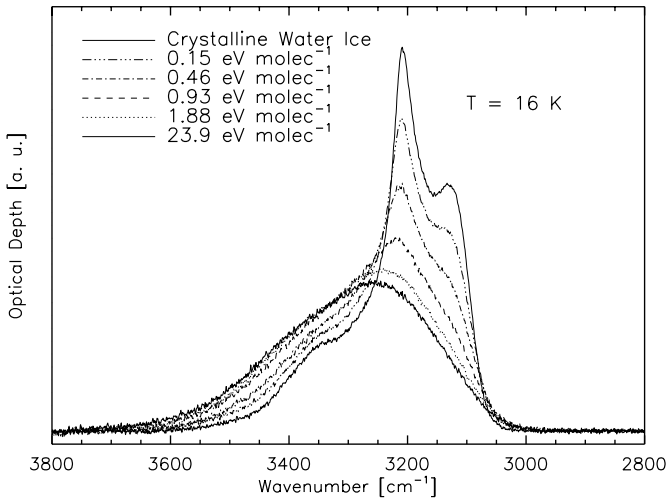


**Fig. 5.** Evolution of the crystalline water ice band under 30 keV $H^+$ ions irradiation.

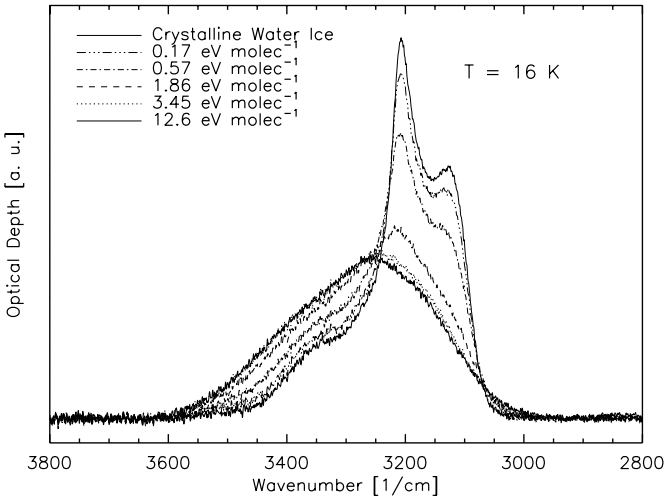


**Fig. 6.** Crystalline $H_2O$ irradiated by 60 keV $Ar^{++}$.

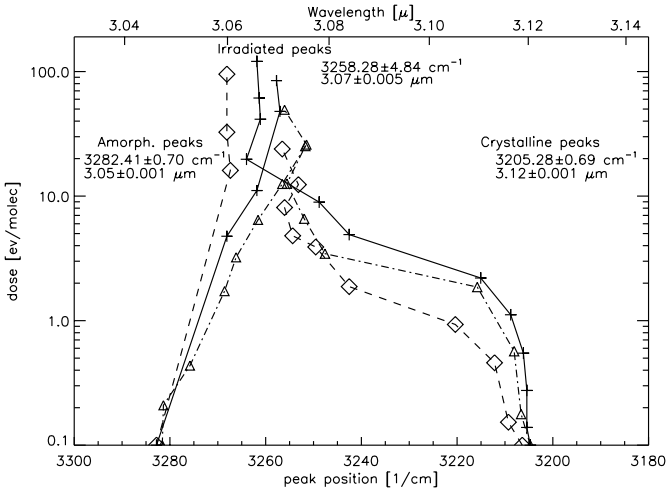


**Fig. 7.** Evolution of the 3-micron band peak position under Ion irradiation and UV photolysis. Diamonds, triangles, and plus symbols are used in the case of 30 keV $H^+$, 60 keV $Ar^{++}$ , and UV Ly-$\alpha$ photons respectively. The mean value and the standard deviation are also displayed for ASW, Ic, and irradiated peak position.

This result can be interpreted as an indication that the Ic sample was amorphized by Lyman-$\alpha$ UV photolysis. From Fig. 4 it is also evident that irradiated ices are slightly different (because of different chemical and/or lattice structure) compared to the as deposited amorphous water ice.

### *4.2. Ion irradiation*

It has been already shown that Ic water ice is efficiently amorphized by fast ion irradiation (Baratta et al. 1991; Strazzulla et al. 1992; Moore et al. 1992) here we confirm the results previously reported with new experiments conducted using different ions/energy values. Figures 5 and 6 show the evolution of the 3-micron band of Ic ice in the case of irradiation with 30 keV $H^+$ and 60 KeV $Ar^{++}$ ions.

In both cases there is a clear profile evolution towards the amorphous shape with increasing irradiation dose. After a few eV/molecule the profile modification is almost complete. As already observed for UV photolysis, the 3-micron band profiles of ion irradiated Ic and amorphous ices are the very same.

## 5. Discussion

The evolution of the peak position of the 3 $\mu$m band under irradiation is shown in Fig. 7 for 30 keV $H^+$, 60 keV $Ar^{++}$ and UV Ly-$\alpha$ photons. A clear trend of the peak position to move towards a region at about 3258 cm$^{-1}$ is observed during both ion irradiation and UV photolysis; this regardless of the fact that the starting point is an amorphous or a crystalline ice. In fact, with the only exeption of 30 keV $H^+$ on ASW, all peaks ended within 5 cm$^{-1}$ (one standard deviation) from the mean peak position value (3258 cm$^{-1}$). We interpret the observed common trends as an evidence that Ic ice amorphize under UV photolysis or ion irradiation. Baragiola et al. (2002) have recently reported a decrease in the porosity of amorphous water ice under ion irradiation at temperatures below 100 K. This finding could

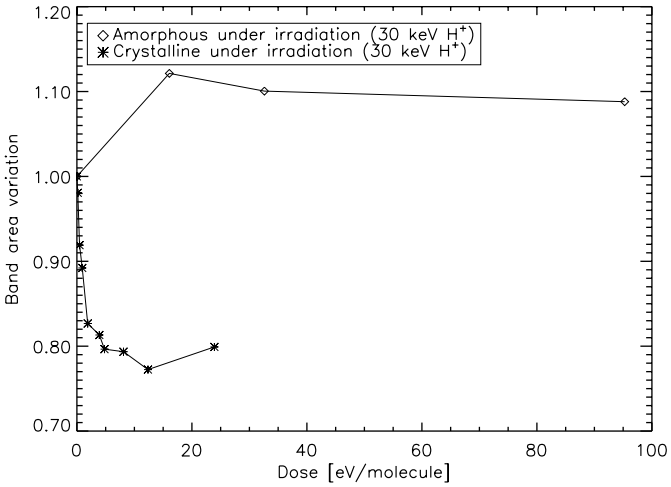


**Fig. 8.** Area variation of the 3 $\mu$ band under 30 keV $H^+$ ions, area values are ratioed to the initial value before irradiation.

be in agreement with the slight 3-micron band profile modification observed for irradiated amorphous water ice.

In Fig. 8, the normalized 3-micron band area of Ic and amorphous water ice irradiated with $H^+$ is plotted versus the irradiation dose. The total absorbance of the band decreases, for Ic ice, as the amorphization proceeds. The final value is about 20% lower than the starting Ic value. On the other hand, the 3-micron band area of amorphous water ice increases by 10%. This effect has also been observed for $He^+$, and $Ar^{++}$. In order to verify if the observed band area variation were in agreement with the hypothesized amorphization effect, we made two different experiments: in the first experiment we acquired IR spectra after deposition at 16 K and after warming up to 150 K; in the second experiment we aquired spectra after deposition at 150 K, after cooling at 16 K and after warming back to 150 K. The spectra of Ic ice samples at 150 K obtained in the two experiments were used to scale the area data of the second experiment to the column density (water molecules/cm$^2$) of the first. The combined results are summarized in Table 1.

Under our standard vacuum condition the background water vapor deposition rate is quite low (less than 0.25 Å/min); in the worst case (60 min) this would give a neglectable (15 Å) contribution to the 3-micron band area for the 800 Å ice films considered in Table 1. This circumstance has been verified in the second (the longest) experiment by noting that the starting Ic band area at 150 K is equal, within 2 percent, to that obtained at the end of the experiment after cooling to 16 K, followed by warming up to 150 K (120 min elapsed).

If an ASW ice layer gives a band area of 100 cm$^{-1}$ at 16 K (in an optical depth scale); an Ic layer of the same column density at the same temperature would have a band area of 136 cm$^{-1}$ (see Table 1). The band areas of both ASW and Ic vary under irradiation (see Fig. 8). We can estimate that the ASW area after irradiation would increase to $100 \times 1.1 = 110$ cm$^{-1}$ (+10%), whether the Ic area would decrease to $136 \times 0.8 = 109$ cm$^{-1}$ (−20%), leading to an almost equal band area for Ic and ASW irradiated ices. The fact that the band area of the irradiated amorphous is almost the same of that of the irradiated Ic ice (for the same column density) implies that both

**Table 1.** Absorbance area variation of the 3 $\mu$m water ice band with temperature, the column density is fixed, ASW as deposited area at 16 K is assumed to be 100.

| Water ice form | Temperature [K] | Absorbance band area |
|---|---|---|
| ASW | 16 ± 1 | 100 |
| Ic [a] | 150 ± 1 | 125 ± 1 |
| Ic [b] | 16 ± 1 | 136 ± 1 |

[a]Ic obtained after warming up to 150 K the ASW film deposited at 16 K (first raw).
[b]Ic obtained by direct deposition at high temperature (150 K), cooled to 16 K.

ices have the same band strength. This strongly supports the hypothesis that Ic and amorphous ices have very similar structures after irradiation. We could not verify if this behavior is also observed for the UV case due to the higher background deposition rate of water during photolysis with the UV lamp and to the longer time needed to reach a given dose compared to the ion irradiation case. Since in UV experiments the deposited samples are thinner than the ion irradiation experiments, the total amount of the additional water ice deposited becomes a significant part of the sample. In particular, for the UV case, the 3-micron band area monotonically increases during photolysis except for the first dose value during the experiment on Ic, where a moderate decrease (5 percent) is observed. By comparing Figs. 3 with 5 we estimate that an additional layer (15% in thickness) of UV photolyzed amorphous water ice was deposited during photolysis.

The efficiency of the process under UV photolysis and ion irradiation can be directly compared by looking at Figs. 3, 5, and 6. In the $H^+$ case an irradiation dose slightly greater than 2 eV per water molecule is enough to almost complete the amorphization process, whereas in the $Ar^{++}$ case it is 3.5 eV per water molecule. For UV photolysis the corresponding value of dose can be estimated to be 5 eV per water molecule.

In order to give a rough estimate of the cross-section of the amorphization process for the different cases we have analyzed the spectra of each experiment by using a simple bilinear fit. By assuming that, in first approximation, at each stage of irradiation the irradiated ice can be described by two coexisting phases (crystalline and irradiated amorphous) with varying volume fraction; we can write the relation:

$$S = F_{\rm a} \times S_{\rm irr\ ASW} + F_{\rm Ic} \times S_{\rm Ic} \quad (1)$$

where $S$ is the sample spectrum (optical depth versus wavenumbers), $F_{\rm a}$ is the irradiated amorphous fraction, $F_{\rm Ic}$ is the cubic residual fraction, while $S_{\rm irr\ ASW}$ and $S_{\rm Ic}$ are the reference spectra of Ic and the irradiated amorphous, respectively (further details in Strazzulla et al. 1992). For each experiment we have performed a fit using Eq. (1) at each irradiation dose, the resulting $F_{\rm a}$ is plotted versus the corresponding dose in Fig. 9, where the solid lines are exponential fits to the data

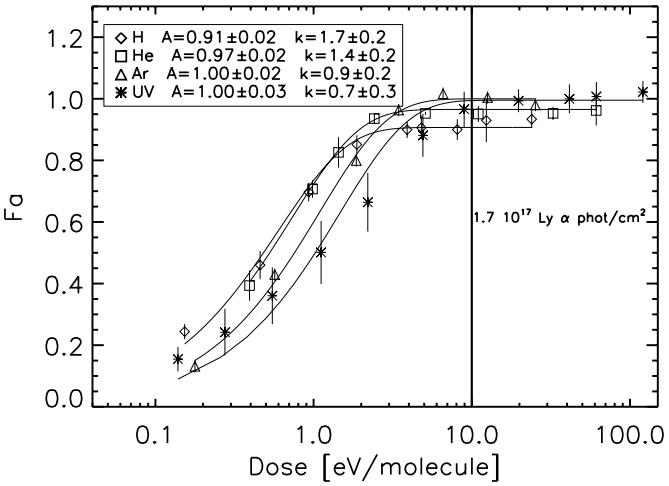


**Fig. 9.** Evolution of the amorphous fraction under ion/photon irradiation at 16 K, $F_a = 1$ means 100% amorphous, the equivalent fluence for the dose value of 10 eV/molecule is also displayed.

points obtained by using the relation:

$$F_a = A \times \left(1 - e^{-kD}\right) \quad (2)$$

where $A$ is the asymptotic amorphous fraction, $D$ is the dose [eV/molecule], and $k$ is the cross-section expressed in molec/eV. The $1/k$ value gives the average energy needed per molecule to transform the Ic water ice in what we have called irradiated amorphous water ice.

From Fig. 9 it is evident that in addition to the already noted higher efficiency of ions compared to that of UV photons, slight differences exist also between different ions in the amorphization process. In particular although 30 keV $H^+$ and 30 keV $He^+$ have similar $k$ values (1.66, 1.38 respectively), 60 keV $Ar^{++}$ ions exhibit a lower cross-section (0.92). The lower efficiency of Ar ions compared to H and He ions could be related to the different amount of anelastic (electronic excitations) and elastic (nuclear collisions) energy components absorbed by the target. In particular the ratio between electronic and nuclear stopping power is more than 10 for 30 keV $H^+$ and 30 keV $He^+$ but is less than 0.5 for 60 keV $Ar^{++}$ ions. This implies that in the case of Ar ions, a significant fraction of energy is released through elastic collisions with the target nuclei, and a fraction of that energy is spent (loss) to excite phonons in the lattice instead of inducing displacements. This could result in a significantly higher efficiency of H and He ions compared to Ar ions in damaging the Ic lattice. In order to verify this hypothesis we got a rough estimate of the energy spent to excite phonons by using the TRIM Montecarlo simulation program. We found that the fraction of energy spent in phonons is 1%, 6% and 38% for 30 keV $H^+$, 30 keV $He^+$ and 60 keV $Ar^{++}$, respectively. Hence, by considering only the energy released that either induces electronic excitations or displacements we can correct the cross-section as: $1.66/(1-0.01) = 1.68$ molec/eV for $H^+$, $1.38/(1-0.06) = 1.47$ molec/eV for $He^+$ and $0.92/(1-0.38) = 1.48$ molec/eV for $Ar^{++}$. The spread among the new cross-sections is significantly lower than before and this supports our hypothesis. In any case we want to stress that both fast ions and UV photons have comparable efficiency (within a factor of 2.5) in amorphizing crystalline water ice. Since the estimated value of $k$ is 0.68 molec/eV for photons, a single Lyman-$\alpha$ (that carries 10.2 eV) may induce the depletion of about 7 ($10.2 \times 0.68$) water ice molecules from the cubic lattice. This is not surprising since every molecule is coordinated with the neighbors in the lattice. Each oxygen atom has four nearest-neighbor oxygen atoms arranged in a tetrahedral pattern, with a single H atom between each near-neighbor oxygen pair. Each oxygen is chemically bonded to two H atoms and is hydrogen bonded to two others. The photodissociation of a single water molecule, breaking and reformation of bonds, formation of radicals or other species such as $H_2O_2$, affects the unit cell of the crystalline structure, hence a larger number of molecules are affected.

The results here discussed are in agreement, from a qualitative point of view, with the only previous work on this topic by Kouchi & Kuroda (1990); UV photons do amorphize a pristine cubic water ice sample. However, as already outlined (see Jenniskens et al. 1995) the Kouchi & Kuroda (1990) result suffered from some quantitative mistakes. In fact, here we have shown that the cross section for Lyman-$\alpha$ induced amorphization is five orders of magnitude lower (i.e. greater dose needed) than that reported by Kouchi & Kuroda (1990) and is of the same order of magnitude measured for fast ions.

## 6. Summary and conclusions

In this paper we report experiments on the effect induced by UV photolysis of water ice samples. To probe the evolution of the samples we have used IR spectroscopy of the 3 $\mu$m band. We also quantitatively compare the results with those of similar experiments conducted in the same experimental setup irradiating with 30 keV $H^+$, 30 keV $He^+$, and 60 keV $Ar^{++}$ ions. We have demonstrated that UV Lyman-$\alpha$ photons are able to amorphize crystalline water ice. The comparison of the efficiency of UV Lyman-$\alpha$ photons and fast ions to amorphize Ic water ice reveals that they are close within a factor of two. In all the cases studied, the amorphization of the Ic ice sample is reached for doses greater than a few eV/molec. We estimate that the efficiency of UV photons to amorphize the ice is slightly lower than the one of the 30 keV $H^+$ ions. In fact, a smaller dose (eV/molecule) is necessary to reach the same amorphization stage in the case of the ion irradiation compared to the UV case (cf. Figs. 5 and 3).

This study has important astrophysical implications. Photons and fast ions are both present in space: they can induce variations in the profile of the 3-micron band of crystalline water ice; therefore these effects have to be considered when one attempts to deduce, from the profile of observed ice bands, information on the temperature history of the responsible dust.

*Acknowledgements.* We are grateful to F. Spinella for his valuable support in the laboratory. This research has been financially supported by the Italian Space Agency (ASI). We also would like to thank the anonymous referee for careful reading and suggestions which have been very helpful in making this paper more clear.

## References


Baratta, G. A., Leto, G., Spinella, F., Strazzulla, G., & Foti, G. 1991, A&A, 252, 421

Baratta, G. A., & Palumbo, M. E. 1998, JOSA A, 15, 3076

Baratta, G. A., Palumbo, M. E., & Strazzulla, G. 2000, A&A, 353, 1045

Baratta, G. A., Leto, G., & Palumbo, M. E. 2002, A&A, 384, 343

Baragiola, R. A., Bahr, D. A., Sekar, K., et al. 2002, Proc. of 27$^{th}$ General Assembly of European Geophysical Society, Nice (France), in press

Boutron, P., & Alben, R. 1975, J. Chem. Phys., 62, 4848

Devlin, J. P. 2001, J. Geophys. Res., 106, E12, 33333

Dubochet, J., & Lepault, J. 1984, J. Phys. France, 45, 85

Gerakines, P. A., Moore, M. H., & Hudson, R. L. 2000, A&A, 357, 793

Gerakines, P. A., Schutte, W. A., & Eherenfreund, P. 1996, A&A, 312, 289

Groth, W. 1937, Z. Phys. Chem., 37, 307

Hagen, W., Tielens, A. G. G. M., & Greenberg, G. 1983, A&AS, 51, 389

Heide. H. G. 1984, Ultramicroscopy 14, 271

Jenniskens, P., Blake, D. F., Wilson, M. A., & Pohorille, A. 1995, ApJ, 455, 389

Kouchi, A., & Kuroda, T. 1990, Nature, 344, 134

Lepault, J., Freeman R., & Dubochet, J. 1984, J. Microsc., 132, RP3-4

Moore, M. H., & Hudson, R. L. 1992, ApJ, 401, 353

Schmitt, B., Greenberg, J. M., & Grim, R. J. A. 1989, ApJ, 340, L33

Smith, M. A. H., Rinsland, C. P., Fridovich, B., & Rao, K. N. 1985, in Molecular spectroscopy: Modern Research. Vol III, ed. K. N. Rao (Academic Press., London), p. 111

Strazzulla, G., Baratta, G. A., Leto, G., & Foti, G. 1992, Europhys. Lett., 18, 517

Warren, S. G. 1984, Appl. Opt., 23, 1206

Westley, M. S., Baratta, G. A., & Baragiola, R. A. 1998, J. Chem. Phys., 108, 3321